ROBUST BLIND SPIKES DECONVOLUTION

Yuejie Chi

Department of ECE and Department of BMI
The Ohio State University, Columbus, Ohio 43210

ABSTRACT

Blind spikes deconvolution, or blind super-resolution, deals with the problem of estimating the delays and amplitudes of spikes from its convolution with an unknown low-pass point spread function. By constraining the point spread function in a known low-dimensional subspace, a convex optimization algorithm called AtomicLift has been proposed to exactly recover the spikes up to an unavoidable scaling ambiguity in the noiseless setting. This paper analyzes the performance of AtomicLift in the presence of bounded noise, and shows that the spikes are localized in a stable manner where the localization inaccuracy is proportional to the noise level. Moreover, we show AtomicLift is also capable to handle sparse outliers in the frequency domain.

***Index Terms*—** blind spikes deconvolution, atomic norm, spectrum estimation

1. INTRODUCTION

Blind spikes deconvolution, or blind super-resolution, deals with the problem of estimating the delays and amplitudes of spikes within a unit interval $[0, 1]$ from its convolution with an unknown low-pass point spread function with a cut-off frequency f_c. This problem naturally arises in applications such as estimating the firing time of neurons whose characteristic function is not known, estimating sparse channel coefficients without transmitting training pilots, and, maybe less obviously, self-calibration of uniform linear arrays.

Unlike the problem of spikes deconvolution with a known point spread function [1], its blind counterpart is much more ill-posed. Further assumptions are usually desirable either on the spike signal or the point spread function to make the problem identifiable, e.g. by assuming they satisfy generic sparsity or subspace constraints [2]. In many applications, the point spread function may be well-modeled as lying in a low-dimensional subspace, which is either known by design, or learned using training data. Under this constraint, to estimate the point spread function one only needs to estimate its orientation in the subspace, which has a much smaller degrees of freedom. The spike signal, on the other hand, normally does not live in an *a priori* determined subspace, or even a finite union of subspaces, since the location of the spikes can be arbitrary. Rather, the spike signal shall be viewed as a sparse signal in a continuous dictionary with an infinite number of atoms.

Motivated by recent advances in atomic norm minimization [3–7], together with the trick of lifting a bilinear inverse problem to a linear underdetermined problem [8–10], an algorithm called *AtomicLift* is developed in [11] for blind spikes deconvolution when the point spread function lies in a known low-dimensional subspace in the noiseless setting. Specifically, AtomicLift is an atomic norm minimization algorithm that motivates joint spectral sparsity among all matrices that satisfy the measurements. Under mild randomness assumptions of the subspace and a minimum separation between spikes by $2/f_c$, AtomicLift admits exact recovery of the spike signal up to an unavoidable scaling factor as soon as the cut-off frequency f_c is on the order of $\mathcal{O}(K^2L^2)$, where K is the number of spikes, and L is the subspace dimension of the point spread function.

In this paper, we analyzes the performance of AtomicLift in the presence of bounded noise. We first propose a natural extension of the algorithm in [11] to handle bounded noise, where we seek a matrix with minimum atomic norm that satisfies the measurements up to the noise level. Two procedures are described for spike localization. The first procedure is to identify peaks of a dual polynomial constructed using the dual solution of AtomicLift, and the second procedure is to apply conventional spectrum estimation methods such as MUSIC [12] to the top left singular vector of the primal solution of AtomicLift. Without exact knowledge of the model order K, both procedures may yield spurious spikes in the estimates. Nonetheless, we prove that the localization inaccuracy of the first procedure is proportional to the noise level, demonstrating the robustness of AtomicLift in the noisy setting. Our analysis is inspired by [13] that quantifies support recovery accuracy in super-resolution using total variation minimization. Numerically, we observe both procedures achieve comparable performance for spikes localization. Finally, we demonstrate that AtomicLift is also robust to sparse outliers in the frequency domain, which can be used to model excessively large gains of antennas during the self-calibration of unitary linear arrays, or harmonic interference in the time-domain signal. Here, AtomicLift seeks a matrix that minimizes the sum of its atomic norm and the ℓ_1 norm of the residual. Numerical examples are provided to show the effectiveness of the proposed approach.

The rest of the paper is organized as below. Section 2 describes the problem formulation of blind spikes deconvolution, and AtomicLift in the noiseless setting. Section 3 analyzes the performance of AtomicLift in the setting with bounded noise. Section 4 generalizes AtomicLift to handle sparse outliers. Numerical examples are provided in Section 5 and we conclude in Section 6. Throughout the paper, bold letters are used to denote matrices and vectors, and unbolded letters to denote scalars. The transpose is denoted by $(\cdot)^T$, the complex conjugate is denoted by $(\cdot)^*$, and the conjugate transpose is denoted by $(\cdot)^H$.

2. BACKGROUNDS

Consider the received continuous-time signal $y(t)$ as a convolution between a point spread function $g(t)$ and a spike signal $x(t)$, possi-

This work was partially supported by ONR under grant N00014-15-1-2387, and by NSF under grant CCF-1527456.

bly corrupted by an additive noise $w(t)$:

$$y(t) = \sum_{k=1}^{K} a_k g(t-\tau_k) = x(t) * g(t) + w(t), \tag{1}$$

where $x(t) = \sum_{k=1}^{K} a_k \delta(t-\tau_k)$, $a_k \in \mathbb{C}$ and $\tau_k \in [0,1)$ are the amplitude and delay of the kth spike, $1 \leq k \leq K$, respectively, and K is the number of spikes. Further denote the set of spike locations as $\mathcal{T} = \{\tau_k\}_{k=1}^{K}$.

Typically, the time resolution of $g(t)$ is constrained, and can be quantified by its maximum cut-off frequency, denoted as f_c. The discrete Fourier transform (DFT) of (1) can be written as

$$\begin{aligned} y_n &= g_n \cdot x_n + w_n \\ &= g_n \cdot \left(\sum_{k=1}^{K} a_k e^{-j2\pi n \tau_k} \right) + w_n, \quad n = -f_c, \ldots, f_c \end{aligned} \tag{2}$$

where $x_n = \sum_{k=1}^{K} a_k e^{-j2\pi n \tau_k}$, g_n and w_n are the nth DFT sample of $g(t)$ and $x(t)$, respectively. In the matrix form, we rewrite (2) as

$$\boldsymbol{y} = \operatorname{diag}(\boldsymbol{g})\boldsymbol{x} + \boldsymbol{w}, \tag{3}$$

where $\boldsymbol{y} = [y_{-f_c}, \ldots, y_{f_c}]^T$, $\boldsymbol{x} = [x_{-f_c}, \ldots, x_{f_c}]^T$, $\boldsymbol{g} = [g_{-f_c}, \ldots, g_{f_c}]^T$, and $\boldsymbol{w} = [w_{-f_c}, \ldots, w_{f_c}]^T$. Interestingly, (3) is also related to blind calibration for uniform linear arrays, where $\boldsymbol{g}$ can be interpreted as the vector of antenna gains. We are interested in estimating the set of spikes $\mathcal{T}$ with their corresponding amplitudes up to an unavoidable scaling ambiguity from $\boldsymbol{y}$.

We now review the AtomicLift algorithm proposed in [11] in the noiseless setting, where $w_n = 0$. To make blind spikes deconvolution more tractable, it is common to exploit additional structures of the point spread function. One popular approach is to assume the point spread function lies in certain low-dimensional subspace, given as

$$\boldsymbol{g} = \boldsymbol{B}\boldsymbol{h},$$

where $\boldsymbol{B} \in \mathbb{C}^{(2f_c+1)\times L}$ is known, but its orientation in the subspace $\boldsymbol{h} \in \mathbb{C}^L$ is unknown. Also, $L \ll (2f_c+1)$. In [11], the author applied the lifting trick [8–10] to rewrite (2) as

$$y_n = \boldsymbol{b}_n^T \boldsymbol{h} x_n = \boldsymbol{b}_n^T \boldsymbol{h} \boldsymbol{e}_n^T \boldsymbol{x} = \boldsymbol{e}_n^T (\boldsymbol{x}\boldsymbol{h}^T)\boldsymbol{b}_n = \boldsymbol{e}_n^T \boldsymbol{Z}^\star \boldsymbol{b}_n, \tag{4}$$

where $\boldsymbol{b}_n \in \mathbb{C}^L$ is the nth column of the matrix $\boldsymbol{B}^T$, and $\boldsymbol{e}_n$ is the nth standard basis vector of $\mathbb{R}^N$. Denote $\boldsymbol{Z}^\star = \boldsymbol{x}\boldsymbol{h}^T$, then (4) can be regarded as a linear measurement of $\boldsymbol{Z}^\star$. Similar, $\boldsymbol{y}$ can be regarded as a set of linear measurements of $\boldsymbol{Z}^\star$, given as

$$\boldsymbol{y} = \mathcal{X}(\boldsymbol{Z}^\star), \tag{5}$$

where $\mathcal{X} : \mathbb{C}^{(2f_c+1)\times L} \mapsto \mathbb{C}^{2f_c+1}$ denotes the operator that performs the linear mapping (4). Since $\boldsymbol{Z}^\star$ can be regarded as a signal ensemble where each column signal is composed of K complex sinusoids with the same frequencies,

$$\boldsymbol{Z}^\star = \boldsymbol{x}\boldsymbol{h}^T = \sum_{k=1}^{K} \tilde{a}_k \boldsymbol{c}(\tau_k)\boldsymbol{h}^T \in \mathbb{C}^{(2f_c+1)\times L},$$

where $\tilde{a}_k = (2f_c+1)^{1/2} a_k$ and

$$\boldsymbol{c}(\tau) = \frac{1}{\sqrt{(2f_c+1)}} \left[e^{j2\pi f_c \tau}, \ldots, 1, \ldots, e^{-j2\pi f_c \tau} \right]^T$$

represents a complex sinusoid with frequency $\tau \in [0,1)$. It is then proposed in [11] to recover $\boldsymbol{Z}^\star$ using the following convex optimization algorithm, denoted as *AtomicLift*,

$$\hat{\boldsymbol{Z}} = \underset{\boldsymbol{Z} \in \mathbb{C}^{(2f_c+1)\times L}}{\operatorname{argmin}} \ \|\boldsymbol{Z}\|_{\mathcal{A}} \quad \text{s. t.} \quad \boldsymbol{y} = \mathcal{X}(\boldsymbol{Z}), \tag{6}$$

where $\|\boldsymbol{Z}\|_{\mathcal{A}}$ is defined in [6] as

$$\|\boldsymbol{Z}\|_{\mathcal{A}} = \inf_{\substack{\tau_k \in [0,1) \\ \boldsymbol{u}_k \in \mathbb{C}^L : \|\boldsymbol{u}_k\|_2 = 1}} \left\{ \sum_k c_k \middle| \boldsymbol{Z} = \sum_k c_k \boldsymbol{A}(\tau_k, \boldsymbol{u}_k), c_k \geq 0 \right\},$$

to motivate joint spectral sparsity, where the atomic set $\mathcal{A}$ contains the set of atoms:

$$\mathcal{A} = \left\{ \boldsymbol{A}(\tau, \boldsymbol{u}) = \boldsymbol{c}(\tau)\boldsymbol{u}^H \in \mathbb{C}^{(2f_c+1)\times L} | \tau \in [0,1), \|\boldsymbol{u}\|_2 = 1 \right\}.$$

Since $\|\boldsymbol{Z}\|_{\mathcal{A}}$ admits an equivalent semidefinite programming (SDP) characterization [6]:

$$\|\boldsymbol{Z}\|_{\mathcal{A}} = \inf_{\substack{\boldsymbol{u} \in \mathbb{C}^{2f_c+1} \\ \boldsymbol{W} \in \mathbb{C}^{L\times L}}} \left\{ \frac{1}{2} \operatorname{Tr}(\operatorname{toep}(\boldsymbol{u})) + \frac{1}{2} \operatorname{Tr}(\boldsymbol{W}) \middle| \begin{bmatrix} \operatorname{toep}(\boldsymbol{u}) & \boldsymbol{Z} \\ \boldsymbol{Z}^H & \boldsymbol{W} \end{bmatrix} \succeq \boldsymbol{0} \right\},$$

where $\operatorname{toep}(\boldsymbol{u})$ is the Toeplitz matrix with $\boldsymbol{u}$ as the first column, the *AtomicLift* algorithm in (6) can be computed efficiently using off-the-shelf solvers.

3. ATOMICLIFT WITH BOUNDED NOISE

In this section, we propose and analyze a natural extension of AtomicLift in the presence of bounded noise, where the corresponding lifted measurement model (5) becomes

$$\boldsymbol{y} = \mathcal{X}(\boldsymbol{Z}^\star) + \boldsymbol{w}, \tag{7}$$

with $\|\boldsymbol{w}\|_2 \leq \epsilon$ for some $\epsilon > 0$. We consider the following AtomicLift algorithm, which seeks a matrix that minimizes the atomic norm as well as satisfies the measurement constraint as

$$\hat{\boldsymbol{Z}}_{\text{noisy}} = \underset{\boldsymbol{Z} \in \mathbb{C}^{(2f_c+1)\times L}}{\operatorname{argmin}} \ \|\boldsymbol{Z}\|_{\mathcal{A}} \quad \text{s.t.} \quad \|\boldsymbol{y} - \mathcal{X}(\boldsymbol{Z})\|_2 \leq \epsilon. \tag{8}$$

3.1. Spike localization via the dual polynomial

By introducing the dual norm $\|\boldsymbol{Y}\|_{\mathcal{A}}^* = \max_{\tau \in [0,1)} \|\boldsymbol{Y}^H \boldsymbol{c}(\tau)\|_2$, we write the dual problem of (8) as

$$\hat{\boldsymbol{p}} = \underset{\boldsymbol{p} \in \mathbb{C}^{(2f_c+1)}}{\operatorname{argmax}} \ \langle \boldsymbol{p}, \boldsymbol{y} \rangle - \frac{\epsilon}{2} \|\boldsymbol{p}\|_2, \quad \text{s.t.} \quad \|\mathcal{X}^*(\boldsymbol{p})\|_{\mathcal{A}}^* \leq 1,$$

where $\mathcal{X}^*(\cdot)$ is the conjugate operator of $\mathcal{X}(\cdot)$. Constructing the dual polynomial as $\boldsymbol{Q}(\tau) = (\mathcal{X}^*(\hat{\boldsymbol{p}}))^H \boldsymbol{c}(\tau)$, the spikes can then be localized by the peaks of $\|\boldsymbol{Q}(\tau)\|_2$ as

$$\hat{\mathcal{T}} = \{\tau \in [0,1) : \|\boldsymbol{Q}(\tau)\|_2 = 1\} \tag{9}$$

following standard arguments as in [4–7]. Since the support set $\hat{\mathcal{T}}$ might contain many spurious peaks, we can find the coefficients of the spikes by solving another discrete optimization problem based on group sparsity [14]. Let $\boldsymbol{V}_{\hat{\mathcal{T}}} = \left\{ \boldsymbol{c}(\tau) | \tau \in \hat{\mathcal{T}} \right\} \in \mathbb{C}^{(2f_c+1)\times|\hat{\mathcal{T}}|}$ be the Vandermonde matrix composed of atoms with frequencies in $\hat{\mathcal{T}}$. Then $\hat{\boldsymbol{Z}}_{\text{noisy}}$ admits the atomic decomposition $\hat{\boldsymbol{Z}}_{\text{noisy}} = \sum_{i=1}^{|\hat{\mathcal{T}}|} \boldsymbol{c}(\hat{\tau}_i)\hat{\boldsymbol{d}}_i^T$, where $\hat{\boldsymbol{d}}_i$ is the corresponding coefficient vector of each spike.

3.2. Performance guarantee

Under similar assumptions as in the noiselss case [11], we show that the precision of spike localizations is proportional to the noise level. Let the minimum separation Δ between spikes be defined as

$$\Delta = \min_{t_i \neq t_j \in \mathcal{T}} |t_i - t_j|, \tag{10}$$

where the distance is the wrap-around distance on the unit circle. We also assume each row of $\boldsymbol{B}$ is sampled independently and identically from a population F, i.e. $\boldsymbol{b}_n \sim F$, $n = -f_c, \ldots, f_c$. Furthermore, we require F satisfies the following properties:

- *Isotropy property:* We say F satisfies the isometry property if for $\boldsymbol{b} \sim F$, $\mathbb{E}\boldsymbol{b}\boldsymbol{b}^H = \boldsymbol{I}_L$.
- *Incoherence property:* for $\boldsymbol{b} = [b_1, \ldots, b_L]^T \sim F$, there exists a coherence parameter μ such that $\max_{1 \leq i \leq L} |b_i|^2 \leq \mu$ holds.

Define a neighborhood of each spike location as $T_i = \{t : |t - \tau_i| \leq 0.1649/f_c\}$, $T_{\text{near}} = \cup_{i=1}^K T_i$ and $T_{\text{far}} = [0,1] \backslash T_{\text{near}}$. Without loss of generality, we assume $\|\boldsymbol{h}\|_2 = 1$. We have the following theorem whose proof is omitted due to space limits.

Theorem 1. *Let $\boldsymbol{B}$ satisfy the isotropy and incoherence properties, $\|\boldsymbol{h}\|_2 = 1$ and $\Delta \geq 2/f_c$. Then as long as there exists a constant C such that $f_c \geq C\mu K^2 L^2 \log^2(f_c/\delta)$, the solution satisfies*

$$\left| \tilde{a}_k - \left(\sum_{\hat{\tau}_j \in T_k \cap \hat{\mathcal{T}}} \hat{\boldsymbol{d}}_j \right)^T \boldsymbol{h}^* \right| \leq C_1 \epsilon, \tag{11a}$$

$$\sum_{\hat{\tau}_j \in T_k \cap \hat{\mathcal{T}}} \|\hat{\boldsymbol{d}}_j^T\|_2 f_c^2 (\hat{\tau}_j - \tau_k)^2 \leq C_2 \epsilon, \tag{11b}$$

$$\sum_{\hat{\tau}_j \in T_{\text{far}} \cap \hat{\mathcal{T}}} \|\hat{\boldsymbol{d}}_j^T\|_2 \leq C_3 \epsilon. \tag{11c}$$

with probability at least $1 - K\delta$, where C_1, C_2 and C_3 are numerical constants.

Theorem 1 suggests the performance of AtomicLift degenerates gracefully as the noise level increases. First, (11a) guarantees that if we sum up the coefficients of the spikes detected within each neighborhood T_k of a true support τ_k, and then the projection error onto the true coefficient vector is proportional to the noise level ϵ. Second, (11b) guarantees the sum of ℓ_2 norms of the spikes within each neighborhood T_k of a true support τ_k, weighted by its quadratic distance to τ_k, is proportional to the noise level. Together with (11a), this indicates most of the detected spikes within T_k corresponding to large coefficients shall be close to the truth spike τ_k. Finally, (11c) indicates the sum of the ℓ_2 norms of the spikes that are far from the true spike is proportional to the noise level. When the noise level is zero, Theorem 1 recovers the guarantee for the noiseless case, where AtomicLift exactly recovers the spike signal.

3.3. Source localization via MUSIC

The above procedure is standard for retrieving source locations in a general multiple measurement vector problem using atomic norm minimization. However, for our problem, since $\boldsymbol{Z}^\star = \boldsymbol{x}\boldsymbol{h}^T$ is also rank-one, we could extract the top left singular vector of $\hat{\boldsymbol{Z}}_{\text{noisy}}$ as $\hat{\boldsymbol{x}}$, which gives an estimate of $\boldsymbol{x}$ up to scaling ambiguity, and then retrieve the source locations from $\hat{\boldsymbol{x}}$ using conventional spectral estimation methods, e.g. MUSIC [12]. Our numerical examples in Section 5 demonstrate this approach achieves similar performance as the dual polynomial.

4. ATOMICLIFT WITH SPARSE OUTLIERS

In some applications, the measurements in the frequency domain may be corrupted by sparse outliers, whose amplitudes can be arbitrary. We consider the following measurement model:

$$\boldsymbol{y} = \mathcal{X}(\boldsymbol{Z}^\star) + \boldsymbol{s}, \tag{12}$$

where $\boldsymbol{s} \in \mathbb{C}^{2f_c+1}$ is an S-sparse vector. The AtomicLift algorithm is then modified as

$$\hat{\boldsymbol{Z}}_{\text{outliers}} = \underset{\boldsymbol{Z} \in \mathbb{C}^{(2f_c+1)\times L}}{\operatorname{argmin}} \|\boldsymbol{Z}\|_{\mathcal{A}} + \|\boldsymbol{y} - \mathcal{X}(\boldsymbol{Z})\|_1, \tag{13}$$

which seeks a matrix that minimizes the sum of its atomic norm and the ℓ_1 norm of the residual. A sufficient condition for (13) to exactly recover $\boldsymbol{Z}^\star$ is given in the following proposition.

Proposition 1. *$\boldsymbol{Z}^\star$ is the unique optimizer of* (13) *if there exists a dual polynomial $\boldsymbol{Q}(\tau) = (\mathcal{X}^*(\boldsymbol{q}))^H \boldsymbol{c}(\tau)$ that satisfies*

$$\begin{aligned} \|\boldsymbol{Q}(\tau)\|_2 &= 1, \quad \tau \in \mathcal{T}, \\ \|\boldsymbol{Q}(\tau)\|_2 &< 1, \quad \tau \notin \mathcal{T}, \\ q_i &= \textit{sign}(s_i), \quad i \in \textit{supp}(\boldsymbol{s}), \\ |q_i| &< 1, \quad i \notin \textit{supp}(\boldsymbol{s}). \end{aligned}$$

This proposition also suggests how to recover the spike locations as well as the support of the outliers from the dual polynomial, which we'll illustrate in the numerical example.

5. NUMERICAL EXPERIMENTS

We conduct numerical experiments to examine the robustness of AtomicLift in the presence of noise. Without loss of generality, in all numerical experiments, we set the index $n \in \{0, \ldots, N-1\}$, rather than $n \in \{-f_c, \ldots, f_c\}$ as in the previous sections.

5.1. AtomicLift with bounded noise

Let $N = 64$, $K = 6$ and $L = 3$. We first randomly generate the spike locations uniformly at random, respecting the minimum separation $\Delta \geq 1/N$, which is about four times smaller than the theoretical requirement, and generate the coefficients of the spikes with a dynamic range of 10dB and a uniform phase. We next randomly generate the low-dimensional subspace $\boldsymbol{B}$ with i.i.d. standard Gaussian entries, and the coefficient vector $\boldsymbol{h}$ with i.i.d. standard Gaussian entries. We introduce additive white Gaussian noise, where each w_n is i.i.d. generated with $\mathcal{CN}(0, \sigma^2)$. The signal-to-noise ratio (SNR) is defined as $10\log_{10}(\|\mathcal{X}(\boldsymbol{Z}^\star)\|_2^2/(N\sigma^2))$dB. Using a standard tail bound $\mathbb{P}\left(\|\boldsymbol{w}\|_2 \leq \sigma\sqrt{N + \sqrt{2N\log 2N}}\right) \geq 1 - \frac{1}{2N}$ [15], we set $\epsilon := \sigma\sqrt{N + \sqrt{2N\log 2N}}$ in (8). Let SNR$=15$dB. Define the top left singular vector of $\hat{\boldsymbol{Z}}_{\text{noisy}}$ as $\hat{\boldsymbol{x}}$. Fig. 1 compares the source localization accuracy of the two approaches, where (a) and (b) depict the source locations identified using the dual polynomial and the recovered magnitudes; (c) and (d) depict the source locations identified using the MATLAB command `rootmusic`$(\hat{\boldsymbol{x}}, |\hat{\mathcal{T}}|)$ and the recovered magnitudes, where $|\hat{\mathcal{T}}|$ is the number of sources identified in (a). Both procedures achieve similar accuracy in source localization. It can be seen that the dual polynomial overestimates the number of spikes, therefore additional model order selection is still necessary. This may be accomplished by thresholding the coefficients, or using classical order selection principle.

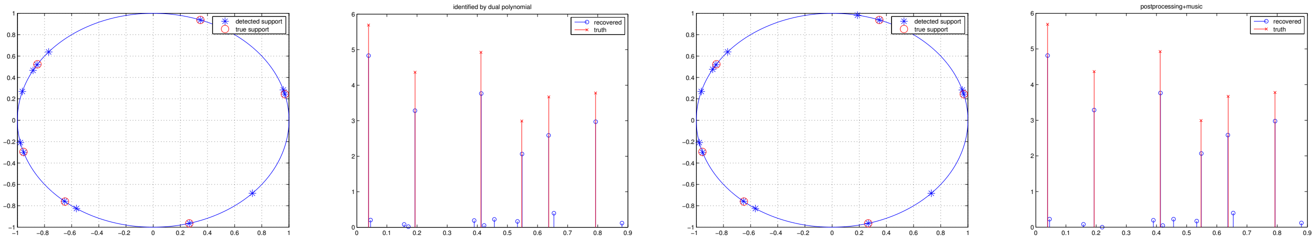

(a) (b) (c) (d)

Fig. 1. Source localization of AtomicLift with bounded noise. (a) and (b): source locations identified using the dual polynomial and the recovered magnitudes; (c) and (d): source locations identified using MUSIC and the recovered magnitudes, when $K = 6$, $N = 64$, $L = 3$ and SNR $= 15$dB.

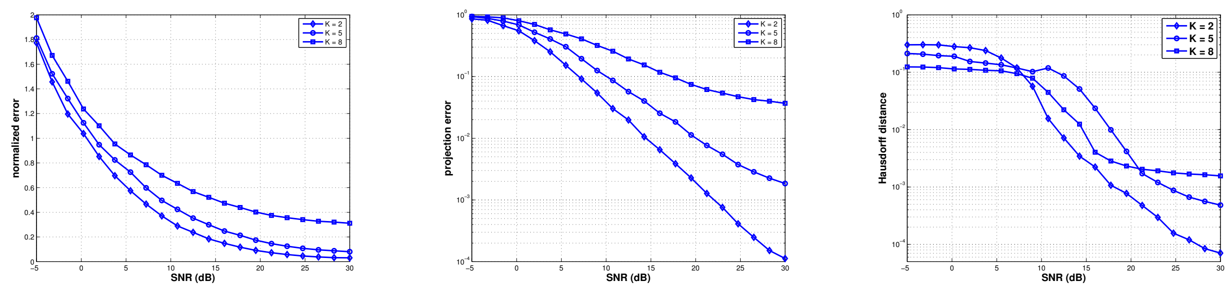

(a) (b) (c)

Fig. 2. The performance of AtomicLift with bounded noise: (a) the normalized error of the recovered $\hat{\boldsymbol{Z}}_{\text{noisy}}$; (b) the projection error of the recovered $\hat{\boldsymbol{x}}$; and (c) the Hausdorff distance between the true spike locations and their estimates, with respect to the SNR when $N = 64$, $L = 3$, and $K = 2, 5, 8$.

We next examine the sensitivity of the performance of source localization with respect to the SNR for various K. For each simulation, we compute the normalized error $\|\hat{\boldsymbol{Z}}_{\text{noisy}} - \boldsymbol{Z}^\star\|_{\text{F}}/\|\boldsymbol{Z}^\star\|_{\text{F}}$, where $\hat{\boldsymbol{Z}}_{\text{noisy}}$ is the solution of (8), and its projection error of $\hat{\boldsymbol{x}}$ on $\boldsymbol{x}$ as $|\langle \hat{\boldsymbol{x}}, \boldsymbol{x}\rangle|^2/\|\hat{\boldsymbol{x}}\|^2\|\boldsymbol{x}\|^2$. We then use the MATLAB command $\texttt{rootmusic}(\hat{\boldsymbol{x}}, K)$ to find the source locations, providing the correct model order K. Fig. 2 shows the normalized error of $\hat{\boldsymbol{Z}}_{\text{noisy}}$ in (a), the projection error of $\hat{\boldsymbol{x}}$ in (b), and the Hausdorff distance between the true spike locations and their estimates in (c) with respect to the SNR, averaged over 100 Monte Carlo runs, for various $K = 2, 5, 8$. The performance of AtomicLift degenerates gracefully as the SNR decreases, and as K increases.

5.2. AtomicLift with sparse outliers

We generate the measurements in the same manner as in Section 5.1 except that sparse outliers are add to noiseless measurements whose support is selected uniformly at random and the amplitudes are generated with uniform random variables Unif$[-1/2, 1/2]$ multiplied by the maximum magnitude of the noiseless measurements. We then run the algorithm (13). Fig. 3 shows the localization of spikes using the dual polynomial $\boldsymbol{Q}(\tau) = (\mathcal{X}^*(\hat{\boldsymbol{q}}))^H \boldsymbol{c}(\tau)$ by examining the peaks of $\|\boldsymbol{Q}(\tau)\|_2$ in (a), as well as the localization of the outliers using $\hat{\boldsymbol{q}}$ by examining the peaks of $|\hat{q}_i|$ in (b).

6. CONCLUSIONS

In this paper we analyzed the performance of AtomicLift in the presence of bounded noise for spike localization both theoretically and numerically. It is demonstrated that AtomicLift is stable against noise and inaccuracy in the estimated source locations is proportional to the noise level under mild conditions. In the future, we will examine the robustness of AtomicLift with respect to perturbations in the assumed subspace model of the point spread function, as well as develop performance guarantees of AtomicLift in the presence of sparse outliers.

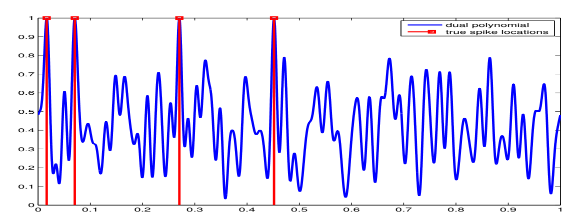

(a) spike localization

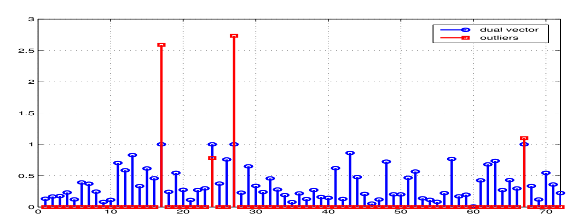

(b) outliers localization

Fig. 3. AtomicLift with sparse outliers. Localization of the spikes and outliers in (a) and (b) with $K = 4$, $S = 4$ and $N = 72$.

7. REFERENCES

[1] E. J. Candès and C. Fernandez-Granda, "Towards a mathematical theory of super-resolution," *Communications on Pure and Applied Mathematics*, vol. 67, no. 6, pp. 906–956, 2014.

[2] Y. Li, K. Lee, and Y. Bresler, "Identifiability in blind deconvolution with subspace or sparsity constraints," *arXiv preprint arXiv:1505.03399*, 2015.

[3] V. Chandrasekaran, B. Recht, P. A. Parrilo, and A. S. Willsky, "The convex geometry of linear inverse problems," *Foundations of Computational Mathematics*, vol. 12, no. 6, pp. 805–849, 2012.

[4] G. Tang, B. N. Bhaskar, P. Shah, and B. Recht, "Compressed sensing off the grid," *IEEE transactions on information theory*, vol. 59, no. 11, pp. 7465–7490, 2013.

[5] Y. Chi and Y. Chen, "Compressive two-dimensional harmonic retrieval via atomic norm minimization," *Signal Processing, IEEE Transactions on*, vol. 63, no. 4, pp. 1030–1042, 2015.

[6] Y. Chi, "Joint sparsity recovery for spectral compressed sensing," in *Acoustics, Speech and Signal Processing (ICASSP), 2014 IEEE International Conference on*. IEEE, 2014, pp. 3938–3942.

[7] Y. Li and Y. Chi, "Off-the-grid line spectrum denoising and estimation with multiple measurement vectors," *arXiv preprint arXiv:1408.2242*, 2014.

[8] A. Ahmed, B. Recht, and J. Romberg, "Blind deconvolution using convex programming," *Information Theory, IEEE Transactions on*, vol. 60, no. 3, pp. 1711–1732, 2014.

[9] S. Ling and T. Strohmer, "Self-calibration and biconvex compressive sensing," *arXiv preprint arXiv:1501.06864*, 2015.

[10] E. J. Candes, T. Strohmer, and V. Voroninski, "Phaselift: Exact and stable signal recovery from magnitude measurements via convex programming," *Communications on Pure and Applied Mathematics*, 2012.

[11] Y. Chi, "Guaranteed blind sparse spikes deconvolution via lifting and convex optimization," *arXiv preprint arXiv:1506.02751*, 2015.

[12] R. Schmidt, "Multiple emitter location and signal parameter estimation," *IEEE Transactions on Antennas and Propagation*, vol. 34, no. 3, pp. 276–280, 1986.

[13] C. Fernandez-Granda, "Support detection in super-resolution," *arXiv preprint arXiv:1302.3921*, 2013.

[14] Y. Eldar and M. Mishali, "Robust recovery of signals from a structured union of subspaces," *IEEE Transactions on Information Theory*, vol. 55, no. 11, pp. 5302 –5316, Nov. 2009.

[15] T. Cai and L. Wang, "Orthogonal matching pursuit for sparse signal recovery with noise," *IEEE Transactions on Information Theory*, vol. 57, no. 7, pp. 1–26, 2011.